



Inhibition of farnesyltransferase with A-176120, a novel and potent farnesyl pyrophosphate analogue

S.K. Tahir, W.-Z. Gu, H.-C. Zhang, J. Leal, J.Y. Lee, P. Kovar, B. Saeed,
S.P. Cherian, E. Devine, J. Cohen, R. Warner, Y.-C. Wang, D. Stout,
D.L. Arendsen, S. Rosenberg, S.-C. Ng*

Cancer Research, Pharmaceutical Product Research Division, Abbott Laboratories, 100 Abbott Park Road, Abbott Park, IL 60064, USA

Received 13 September 1999; received in revised form 2 February 2000; accepted 16 February 2000

Abstract

Farnesylation of Ras is required for its transforming activity in human cancer and the reaction is catalysed by the enzyme farnesyltransferase. Recently, we discovered a novel chemical series of potent farnesyl pyrophosphate (FPP) analogues which selectively inhibited farnesyltransferase. Our most potent compound to date in this series, A-176120, selectively inhibited farnesyltransferase activity (IC_{50} 1.2 ± 0.3 nM) over the closely related enzymes geranylgeranyltransferase I (GGTaseI) (IC_{50} 423 ± 1.8 nM), geranylgeranyltransferase II (GGTaseII) (IC_{50} 3000 nM) and squalene synthase (SSase) ($IC_{50} > 10\,000$ nM). A-176120 inhibited Ras processing in H-ras-transformed NIH3T3 cells and HCT116 K-ras-mutated cells (ED_{50} 1.6 and 0.5 μ M, respectively). The anti-angiogenic potential of A-176120 was demonstrated by a decrease in Ras processing, cell proliferation and capillary structure formation of human umbilical vein endothelial cells (HUVEC), and a decrease in the secretion of vascular endothelial growth factor (VEGF) from HCT116 cells. *In vivo*, A-176120 reduced H-ras NIH3T3 tumour growth and extended the lifespan of nude mice inoculated with H- or K-ras-transformed NIH3T3 cells. A-176120 also had an additive effect in combination with cyclophosphamide in nude mice inoculated with K-ras NIH3T3 transformed cells. Overall, our results demonstrate that A-176120 is a potent FPP mimetic with both antitumour and anti-angiogenic properties. © 2000 Elsevier Science Ltd. All rights reserved.

Keywords: Farnesyltransferase; Farnesyl pyrophosphate analogue; Angiogenesis; Ras processing; Vascular endothelial growth factor; Squalene synthase; Cyclophosphamide; Human tumour xenograft

1. Introduction

As part of our efforts to discover and develop a new hypocholesterolaemic agent based on the inhibition of the enzyme squalene synthase (SSase), we discovered that the 1,3-isomers of our cyclobutane series were potent inhibitors of farnesyltransferase (FTase), but not potent inhibitors of SSase. FTase is a cytosolic enzyme which is known to catalyse the transfer of a farnesyl group from farnesyl pyrophosphate (FPP) to Ras [1,2], a GTP binding protein involved in the regulation of cell growth [3,4]. Mutations of Ras, especially K-Ras, occur in approximately 20–30% of all human cancers, particularly in pancreatic (90%), colon (50%) and lung (30%) carcinomas [5,6]. Ras cycles between an “on”

and “off” state by binding to and hydrolysing GTP to GDP, respectively [7,8]. The cycling of Ras bound to GTP and GDP leads to the regulation of normal cell division. When *ras* mutates, oncogenic Ras mutant proteins lose their intrinsic GTPase activity and they become constitutively bound to GTP. As a consequence, oncogenic Ras proteins are in a perpetual “on state” leading to uncontrolled cell division in the absence of growth signals. Since the first and obligatory step for Ras activity is the addition of a farnesyl group to its carboxy-terminal CAAX motif [1,2], we examined the potential of our FPP farnesyltransferase inhibitors (FTIs) as anticancer therapeutic agents.

There have been several approaches taken to develop FTIs including CAAX carboxyl terminal tetrapeptide analogues, FPP analogues, bisubstrate transition state analogues and natural products found through random screening efforts [9–14]. In this report, we describe the biological characteristics of A-176120, the most potent

* Corresponding author. Tel: +847-937-9635; fax: +847-937-4150.
E-mail address: shi-chung.c.ng@abbott.com (S.-C. Ng).

tricarboxylic acid benzene FPP mimetic inhibitor of FTase developed thus far in this series.

2. Materials and methods

2.1. Chemistry of A-176120

The structures of A-87049 ((1 α ,2 β ,3 β ,4 α)-3,4-bis[[[(4-phenoxyphenyl)methyl]propylamino]carbonyl]-1,2-cyclobutanedicarboxylic acid), A-87050 (2,4-bis[[[(4-phenoxyphenyl)methyl]propylamino]carbonyl]-1,3-cyclobutanedicarboxylic acid), A-88681 (2,4-bis[[[(4-phenoxyphenyl)methyl](phenylmethyl)amino]carbonyl]-1,3-cyclobutanedicarboxylic acid), A-122330 (5-[[[(4-phenoxyphenyl)methyl](phenylmethyl)amino]carbonyl]-1,2,4-benzenetricarboxylic acid), A-181792 (4-[[[(2-ethoxyphenyl)methyl][3-(4-methylphenoxy)phenyl]methyl]amino]carbonyl]-1,2-benzenedicarboxylic acid) and A-176120 (5-[N-(2-ethoxybenzyl)-N-(4-tolyloxy-3-benzyl)aminocarbonyl]benzene-1,2,4-tricarboxylic acid) are shown in Fig. 1.

2.2. Cell culture

Human HCT116 colon carcinoma and MiaPaCa-2 pancreatic carcinoma cells (American Type Culture Collection, ATCC, Rockville, MD, USA) were cultured with Dulbecco's modified Eagle's medium (DMEM), supplemented with 10% fetal bovine serum (FBS) (and 2.5% horse serum for MiaPaCa-2) and 1% antibiotic-antimycotic (Gibco, Grand Island, NY, USA). H- and K-ras-transformed NIH3T3 cells, graciously provided by Dr Channing Der (U. North Carolina, NC, USA), were cultured in DMEM, supplemented with 10% calf serum. Normal human umbilical vascular endothelial cells (HUVEC, Clonetics, San Diego, CA, USA) were cultured on Matrigel® (Collaborative Research, Bedford, MA, USA) with endothelial growth medium (EGM Bulletkit) supplemented with 3% FBS, bovine brain extract (12 μ g/ml), human epidermal growth factor (10 ng/ml), hydrocortisone acetate (1 μ g/ml) and gentamycin-1000 (50 μ g/ml). HCT116, MiaPaCa-2 and HUVEC cell lines were cultured at 37°C in a humidified chamber containing 95% air and 5% CO₂. H- and K-ras-transformed NIH3T3 cells were cultured at 37°C in a humidified chamber containing 90% air and 10% CO₂.

2.3. In vitro enzyme assays

The IC₅₀ values of the FTIs to inhibit bovine brain FTase activity *in vitro* with a substrate fragment were performed using scintillation proximity assay (SPA) technology in a 96-well format. Stock solutions for each compound were prepared in ethanol (1 mM). In each

well, assay buffer (50 mM Hepes, 30 mM MgCl₂, 20 mM KCl, 5 mM DTT, 0.01% Triton X-100, pH 7.0), purified bovine brain FTase, [³H]FPP (NEN, Boston, MA, USA) and a biotin conjugated K-Ras(B) decapeptide (KSKTKCVIM) were added with varying concentrations of each inhibitor. The samples were incubated at 37°C with gentle shaking for 30 min. After the 30 min incubation, the plates were placed on ice, stop/bead reagent was added and the counts associated with the beads were determined using a Packard Top-Count™ Microplate Scintillation Counter (Packard Instrument Company, Meriden, CT, USA).

The IC₅₀ values of the FTIs to inhibit bovine brain FTase, GGTase I and GGTase II activity *in vitro* using an intact protein substrate were performed using a filter binding assay as previously described [15]. Measurement of SSase activity was performed as previously described using SSase purified from rat liver microsomes [16].

2.4. Competitive inhibition assay

A-176120 was tested at various concentrations to determine if it competed either with the Ras peptide or FPP as a substrate for FTase using the [³H]-SPA enzyme assay according to the manufacturer's instructions (Amersham, Arlington Heights, IL, USA).

2.5. Ras processing assay

Approximately 1 \times 10⁵ cells were plated in 25 cm² flasks and allowed to attach overnight. The culture medium was replaced with medium containing A-176120 or vehicle (1% DMSO) and treated for 48 h. Cells were lysed with lysis buffer (Gibco). Proteins from cell lysates were fractionated by 15% sodium dodecyl sulphate polyacrylamide gel electrophoresis (SDS-PAGE) and transferred to nitrocellulose. The blots were incubated in blocking buffer (2% non-fat dry milk, 3% bovine serum albumin) overnight and probed with a pan anti-Ras antibody diluted 1:2000 (Transduction Labs, Lexington, KY, USA). Ras was detected using a horseradish conjugated anti-mouse IgG diluted 1:2000 (Amersham) and visualised by enhanced chemiluminescence (ECL kit, Amersham). The bands were quantified by densitometry using Image-Pro Plus™ (Media Cybernetics, Silver Spring, MD, USA).

2.6. Soft agar colony formation assay

The effect of A-176120 on anchorage-independent growth was tested by plating 3 \times 10⁴ cells in 6-well culture plates in a 0.35% agar layer overlaid on top of a 0.7% agar layer containing DMEM, 10% FBS and the appropriate dilution of A-176120 or vehicle. After 6 h, DMEM supplemented with 10% FBS plus or minus

drug was added to each well and replaced twice a week. After treatment, the colonies were stained with p-iodo-nitrotetrazolium (Sigma, St Louis, MO, USA), photographed using a Sony CCD camera and quantified using Image-Pro Plus.

2.7. HUVEC tube formation assay and proliferation

HUVEC tube formation was assessed as previously described [17]. Briefly, approximately 5×10^5 HUVEC (passages 2–8) in 1 ml of medium were plated onto Matrigel. After 1 h of incubation, another 1 ml of medium with A-176120 or vehicle (1% DMSO) was added to each well. After 12 h, the cell cultures were fixed and stained with Diff-Quik (Baxter, Waukegan, IL, USA), photographed with a Sony CCD camera mounted on a Nikon Diaphot 300 microscope. Tube formation was quantified using Image-Pro Plus by segmenting the cell meshwork based on contrast differences and determining the total pixels (area). The area of tube formation from drug-treated animals was expressed as a per cent of untreated controls.

To assess the effect of A-176120 on HUVEC proliferation and viability, approximately 2.5×10^4 HUVEC were plated on 8-chamber glass slides. After the cells attached, the medium was replaced with fresh medium containing A-176120 or vehicle (1% DMSO). After 12 h, the total number of cells/well was determined using Image-Pro Plus. We assessed toxicity by adding an equal volume of prewarmed propidium iodide (50 $\mu\text{g}/\text{ml}$ propidium iodide in phosphate buffered saline (PBS)) to each well and counting the number of dead cells/well using Image-Pro Plus.

2.8. VEGF secretion

The culture medium collected from HCT116 cells treated with A-176120 was used to evaluate vascular endothelial growth factor (VEGF) secretion. VEGF was measured by quantitative sandwich enzyme immunoassay technique using a quantikine kit (R&D, Minneapolis, MN, USA) according to the manufacturer's instructions and normalised to cell number using the alamarBlue assay. The release of lactate dehydrogenase (LDH) into the culture medium was used to assess the non-specific toxicity of A-176120 on HCT116 cells according to the manufacturer's instructions (Promega, Madison, WI, USA).

2.9. Human tumour xenograft in nude mice

2.9.1. NIH3T3 H-ras tumour model

Male BR nu/nu mice aged 8 weeks (Charles River, ME, USA) were inoculated subcutaneously (s.c.) in the right flank with 0.5 ml of a 1:10 brei of H-ras transformed NIH3T3 cells. Mice were randomly divided into

control ($n=20$) or treatment groups ($n=10$). Alza osmotic minipumps (model 2002, Alzet, Palo Alto, CA, USA) containing A-176120 or vehicle (propylene glycol) were implanted intraperitoneally (i.p.) in each mouse on study day 3. Cyclophosphamide, a positive control, was given by i.p. injection on days 1, 5 and 9. Tumour volume was estimated by measuring the length and width of the tumour mass with digital calipers and by applying the formula $(L \times W^2)/2$. The % increase in lifespan (ILS) was calculated by subtracting the delay in mean time of vehicle control tumours to reach 1 g from the mean time of drug-treated tumours to reach 1 g, divided by the mean time of vehicle-treated tumours to reach 1 g $\times 100\%$ [18]. For humane reasons, all mice were euthanised once the tumours reached at least 1 g. Statistical significance was determined using Student's *t*-test.

2.9.2. NIH3T3 K-ras tumour model

Male BR nu/nu mice were inoculated i.p. with 0.5 ml of a 1:10 brei of K-ras-transformed NIH3T3 cells on day 0. Mice were randomly divided into control ($n=20$) or treatment groups ($n=10$). Alza osmotic minipumps (model 2002, Alzet) containing A-176120 or vehicle (propylene glycol) were implanted i.p. in each mouse on study day 1. Cyclophosphamide, a positive control, was given by i.p. injection on day 1. For combination therapy, mice were treated with cyclophosphamide at 25 mg/kg on study day 1 plus 100 mg/kg/day A-176120 via minipump. The % increase in lifespan (ILS) was calculated by subtracting the delay in mean survival time of vehicle control animals from the mean survival time of drug-treated animals, divided by the mean survival time of vehicle-treated animals $\times 100\%$. Statistical significance was determined using Student's *t*-test.

3. Results

3.1. Design of A-176120

In an effort to determine the selectivity of squalene synthase inhibitors (SSIs) we discovered that certain 1,3-isomers of our cyclobutane series were modest FTIs and weak SSIs (A-87050) (Fig. 1). Conversely, certain 1,2-isomers were potent SSIs and weak FTIs (A-87049). When the *n*-alkyl groups on the nitrogens of A-87050 were replaced by benzyl groups (A-88681), the FTI activity increased and virtually all SSI activity decreased. Incorporating as a core unit benzene-1,2,4,5-tetracarboxylic acid, the tricarboxylic derivative A-122330 was a significantly more potent FTI. Further modifications led to A-176120 which was a significantly more potent FTI than either A-88681 or A-122330.

3.2. A-176120 is a potent and selective FTase inhibitor (FTI) *in vitro*

A-176120 was further tested *in vitro* and *in vivo* since it had the best potency in the *in vitro* FTase assay for this series of compounds. The potency of A-176120 against bovine FTase activity was evaluated using an *in vitro* enzyme assay with the substrates K-Ras(B) decapeptide (KKSKTKCVIM) or intact H-Ras. The concentration of A-176120 to inhibit Ras farnesylation by 50% (IC_{50}) was 1.2 and 2 nM for each FTase substrate, respectively. The activity of A-176120 was 352–(423 nM) and 2500–(3000 nM) fold more selective for FTase over the closely related enzymes GGTase I and GGTase II, respectively. Since FPP is a substrate for SSase, the effect of A-176120 on the activity of this enzyme was assessed to further demonstrate its selectivity. The IC_{50} of A-176120 to inhibit SSase activity was greater than 10000 nM, suggesting that it does not interfere with the activity of SSase, an enzyme important for the biosynthesis of cholesterol.

3.3. Competitive inhibition of FPP with A-176120

Kinetic analysis using variable amounts of either FPP or Ras peptide substrates were performed in order to assess the FPP mimetic or peptidomimetic effect of A-176120, respectively. The ability of A-176120 to compete with the Ras peptide or FPP as a substrate for FTase is shown in Fig. 2(a) and (b), respectively. To investigate the peptidomimetic effect of A-176120, the final peptide concentration was varied, whereas the final concentration of FPP remained constant (0.12 μ M). To investigate the FPP mimetic effect of A-176120, the final

FPP concentration was varied whereas the final concentration of peptide remained constant (0.1 μ M). A-176120 competed with FPP as a substrate for FTase but not with the Ras peptide. The inhibition constant (K_i) of A-176120 to compete with FPP binding was 1.5 nM.

3.4. A-176120 inhibits Ras processing in whole tumour cells

The ability of A-176120 to penetrate and inhibit Ras processing in intact cells was assessed using NIH3T3 H-ras and HCT116 K-ras cells. The cells were treated with varying concentrations of A-176120 for 48 h, lysed and the proteins fractionated by SDS-PAGE. Processed and unprocessed Ras were detected by Western blot analysis using a pan-Ras antibody (Fig. 3). A-176120 inhibited post-translational Ras processing in a dose-dependent manner. The concentration to inhibit Ras processing by 50% (ED_{50}) in NIH3T3 and HCT116 cells was 1.6 and 0.5 μ M, respectively.

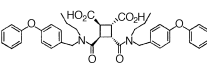
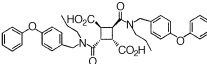
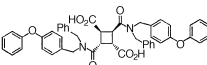
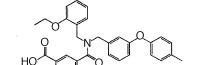
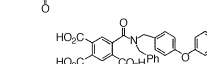
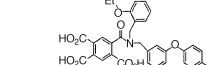
Chemical Structure	Inhibitors	IC_{50} (nM)	
		Bovine SSase	Bovine FTase
	A-87049	37	>10000
	A-87050	1500	4400
	A-88681	>10000	31
	A-181792	no data	14
	A-122330	>10000	7.6
	A-176120	>10000	1.2

Fig. 1. Structure of A-87049, A-87050, A-88681, A-181792, A-122330 and A-176120 and comparison of their farnesyl transferase (FTase) and squalene synthase (SSase) inhibition activity *in vitro*.

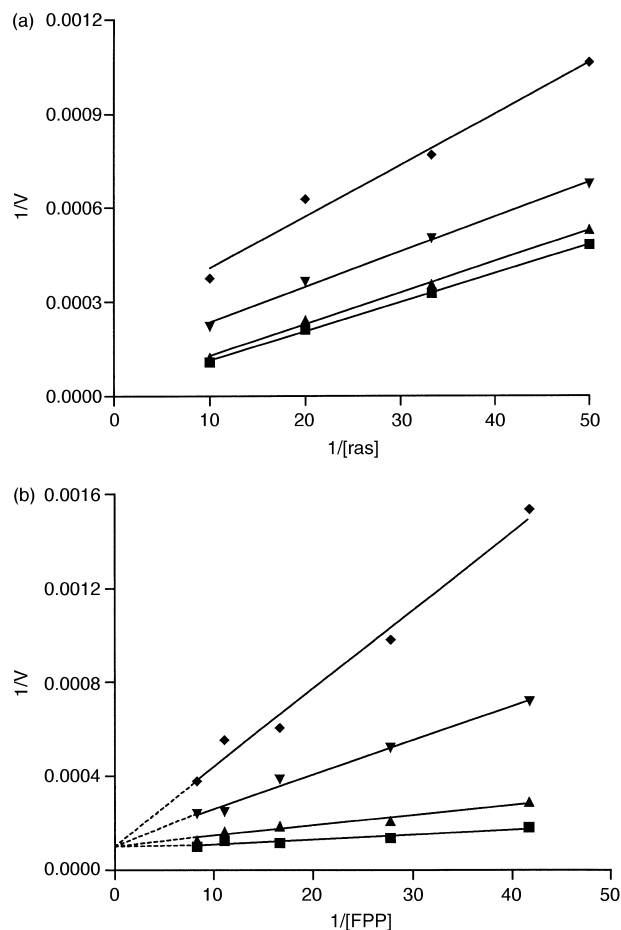


Fig. 2. Competitive inhibition of farnesyl transferase (FTase). Assays were performed using a [3 H]-scintillation proximity (SPA) enzyme assay kit with bovine FTase. (a) Varying Ras peptide and constant farnesyl pyrophosphate (FPP) concentration in the presence of 0 (■), 10 (▲), 20 (▼) or 30 (◆) nM A-176120. (b) Varying FPP and constant Ras peptide concentration in the presence of 0, 10, 20 or 30 nM A-176120. V = velocity.

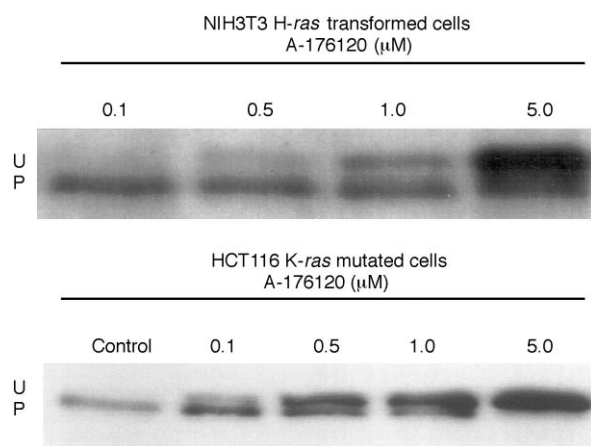


Fig. 3. Post-translational processing of Ras following A-176120 treatment. NIH3T3 H-*ras*-transformed cells and HCT116 cells were treated with varying concentrations of A-176120 for 48 h, lysed and the protein was fractionated on a 15% sodium dodecyl sulphate (SDS)-polyacrylamide gel. Ras was detected by Western blot using a pan-Ras specific antibody. U, unprocessed ras; P, processed ras.

3.5. A-176120 inhibits anchorage-independent human tumour cell growth

Anchorage-independent growth of HCT116 and MiaPaCa-2 cell lines was inhibited by A-176120 (Table

1). We observed that colony formation was inhibited in a dose-dependent manner following treatment with A-176120 in both cell lines. The ED_{50} was 3 and 0.87 μ M for HCT116 and MiaPaCa-2 cells, respectively. We also observed that a reduction in soft agar colony number was accompanied by a reduction in colony size.

3.6. A-176120 inhibits HUVEC tube formation *in vitro*

It has been previously reported that *ras* oncogenes can contribute to tumour development directly by promoting tumour cell proliferation and indirectly by stimulating VEGF-dependent angiogenesis [19]. Therefore, we assessed the anti-angiogenic effects of A-176120 by its ability to inhibit HUVEC tube formation as well as tumour cell VEGF secretion *in vitro*. Tubulogenesis was induced in vascular endothelial cells by plating them onto the surface of Matrigel for several hours. Tube formation of untreated and treated HUVEC when cultured on Matrigel for 12 h are shown in Fig. 4(a). A decrease in both the number and thickness of vessel formation was observed following A-176120 treatment compared with the untreated controls with an effective dose (ED)₅₀ of approximately 3 μ M (Fig. 4b). To test if any FTI would have a similar effect on HUVEC tube formation, we tested A-181792, a structurally similar but weaker FTI (Table 1). We did not observe any effect

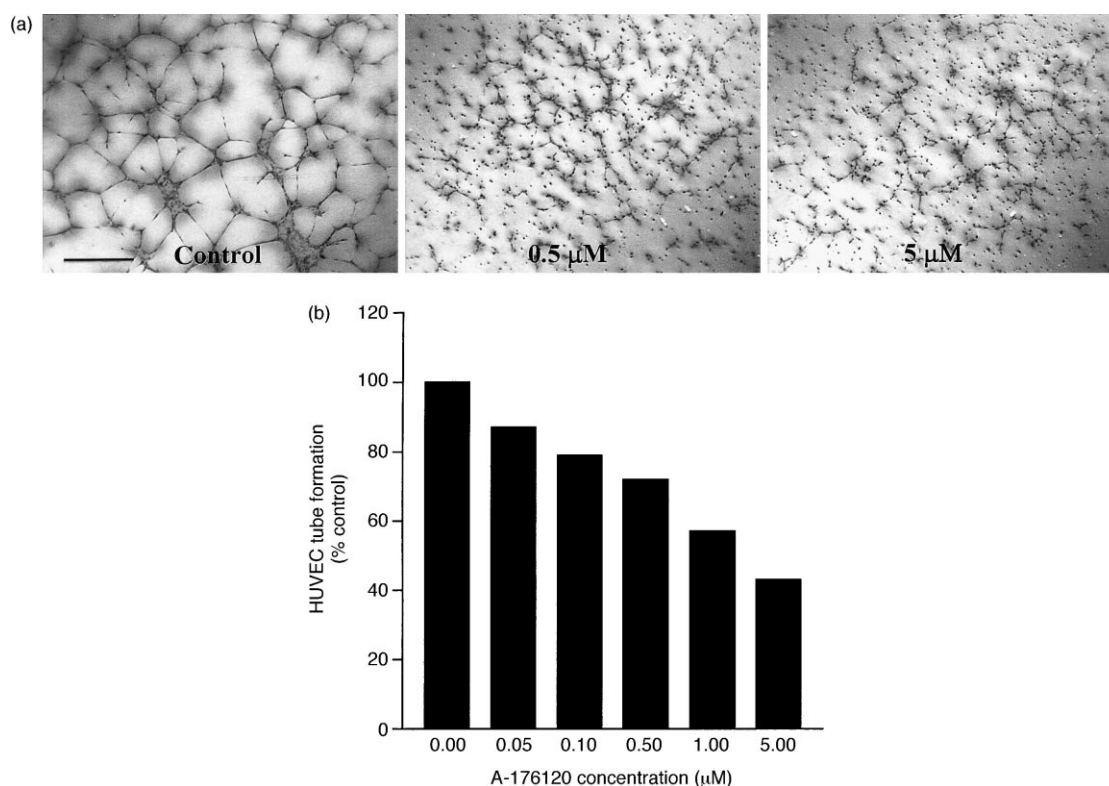


Fig. 4. Effect of A-176120 on human umbilical vein endothelial cells (HUVEC) tube formation. HUVEC were plated onto Matrigel and treated with A-176120 for 12 h and tube formation was quantified using Image-Pro Plus. (a) Representative images of HUVEC following 0, 0.5 and 5 μ M treatment. (b) Quantitative analysis of HUVEC tube formation following drug treatment. Bar = 400 μ m.

Table 1

A-176120 effect on anchorage-independent growth. A soft agar colony formation assay was carried out as in Materials and Methods. After 10–14 days of incubation, colonies from duplicate wells were stained, photographed and quantified

Cell line	Tissue	<i>ras</i> Mutation	EC ₅₀ (μM)
HCT116	colon	K- <i>ras</i>	3.0 (2) ^a
MiaPaCa-2	pancreatic	K- <i>ras</i>	0.87 (2)

^a Number in parentheses represents number of trials.

of A-181792 on HUVEC tube formation at concentrations as high as 25 μM (data not shown).

3.7. A-176120 inhibits HUVEC Ras processing and proliferation in vitro

To test whether A-176120 directly affected HUVEC proliferation and/or Ras processing, we treated the cells with varying concentrations for 12 h. We observed a dose-dependent decrease in Ras processing in HUVEC cells with an ED₅₀ of approximately 5 μM (Fig. 5a). Similarly, we observed a decrease in HUVEC proliferation by approximately 20–30% as assessed by a decrease in total cell number/well (Fig. 5b). The decrease in cell

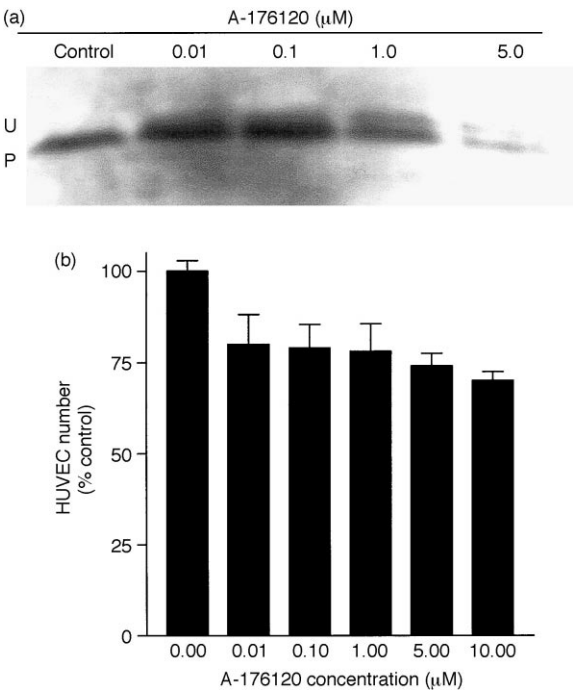


Fig. 5. A-176120 reduced human umbilical vein endothelial cells (HUVEC) Ras processing and proliferation *in vitro*. (a) ras Processing in HUVEC. Cells were treated with varying concentrations of A-176120 for 12 h, lysed and the protein was fractionated on a 15% sodium dodecyl sulphate (SDS)-polyacrylamide gel. Ras was detected by Western blot using a pan-Ras specific antibody. U, unprocessed ras; P, processed ras. (b) Per cent change in HUVEC number. HUVEC were treated for 12 h and the total cell number was determined using Image-Pro Plus. Data represent the mean±standard error, *n* = 3.

number was not due to an increase in cell death since we did not see any difference in the number of propidium iodide-stained cells in the treated and control cells.

3.8. A-176120 reduces HCT116 proliferation and VEGF secretion in vitro

A-176120 reduced anchorage-dependent growth of HCT116 cells in a dose-dependent manner at non-toxic levels (as determined by LDH release) by 0, 5, 23 and 46% following 0.5, 5, 25 and 50 μM treatment for 48 h. VEGF levels released by HCT116 cells (normalised to cell number) declined following A-176120 treatment in a dose-dependent manner. Normalised VEGF levels were reduced by 0, 19, 21 and 52% relative to untreated controls following treatment with 0.5, 5, 25 and 50 μM A-176120 for 48 h, respectively (Fig. 6).

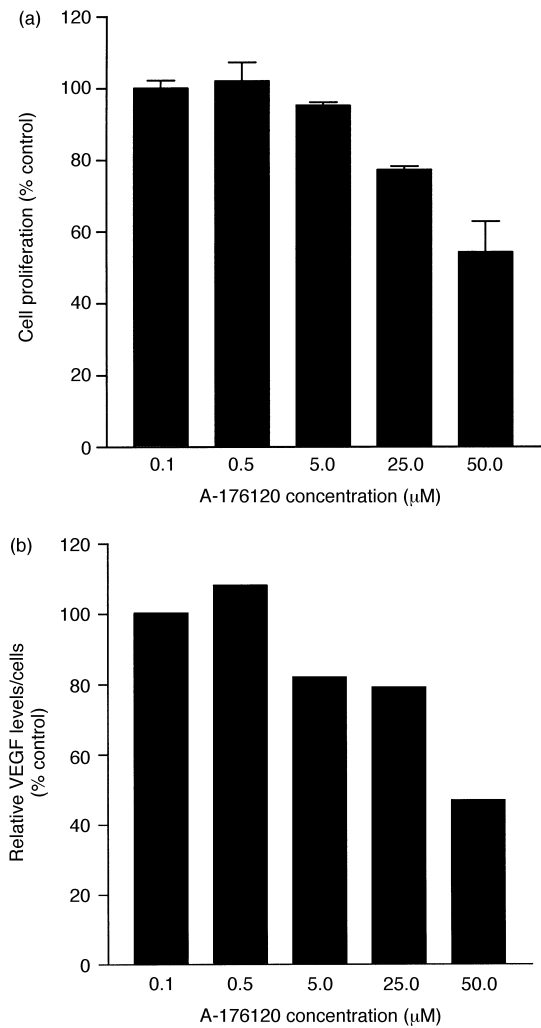


Fig. 6. A-176120 reduced HCT116 anchorage-dependent growth and vascular endothelial growth factor (VEGF) secretion. HCT116 cells treated with varying concentrations of A-176120 for 48 h. (a) Cell proliferation determined using alamarBlue. (b) Normalised VEGF levels/cell secreted into the culture medium by HCT116 cells.

3.9. A-176120 reduces tumour growth in vivo

We examined the *in vivo* efficacy of A-176120 administered i.p. via minipump against mouse H-*ras*-transformed NIH3T3 cells in male nude mice. All nude mice inoculated s.c. with H-*ras* NIH3T3 cells developed palpable tumours within 2 days. Animals were monitored until their tumours reached 1000 mm³ (~1 g) and were sacrificed at that time for humane reasons. The % increase in survival (ILS) was calculated as the % difference in the mean time for drug-treated animal tumours to reach 1 g from the mean time for control animal tumours to reach 1 g [18]. No side-effects (i.e. decrease in body weight or other clinical signs) were observed over the course of the study. The mean control tumour volume on day 17 was 693±190 mm³ and the mean time for the control tumours to reach 1 g was approximately 21 days (Fig. 7a and b, respectively). A-176120 treatment at 50 or 100 mg/kg/day suppressed H-*ras* tumour growth by 57% ($P=0.09$) and 64% ($P=0.07$), respectively, compared with controls on study day 17 (Fig. 7a). The mean delay of H-*ras* NIH3T3 tumours to reach 1 g was increased significantly ($P<0.05$) by 4.2 and 8.5 days following 50 and 100 mg/kg/day A-176120 treatment, which represented an ILS of 20 and 41%, respectively (Fig. 7b). Similarly, cyclophosphamide treatment at 25 or 50 mg/kg/day suppressed H-*ras* tumour growth by 85% ($P<0.05$) and 88% ($P<0.05$) on study day 17, respectively, compared with controls (Fig. 7a). The mean delay in growth of H-*ras* NIH3T3 tumours to reach 1 g following 25 and 50 mg/kg/day of cyclophosphamide treatment was increased significantly by 6.6 and 4.5 days ($P<0.05$, ILS 32 and 22%), respectively (Fig. 7b).

We next examined the *in vivo* antitumour effect of A-176120 on K-*ras* NIH3T3 cells implanted i.p. and treated continuously i.p. by minipump in male nude mice. The mean survival time increased significantly ($P<0.05$) by 3.2 and 3.7 days which represented an ILS of 28 and 33% following 100 and 200 mg/kg/day A-176120 treatment, respectively, and 2 days ($P=0.0551$, ILS of 18%) following 25 mg/kg/day cyclophosphamide i.p. treatment (Fig. 8). The combination treatment of A-176120 and cyclophosphamide was additive in that the mean survival time following 100 mg/kg/day A-176120 with 25 mg/kg cyclophosphamide increased significantly ($P<0.05$) by 5.5 days which represented an ILS of 49%.

4. Discussion

From our results we concluded that A-176120 inhibited Ras farnesylation in a potent and selective manner *in vitro* and it competed with FPP, but not Ras, as a substrate for FTase. The use of FPP mimetics represents one promising strategy to block FTase activity since

FPP is one of the substrates used by FTase to farnesylate Ras. Several groups have reported FPP mimetic inhibitors of FTase, however, A-176120 is the most

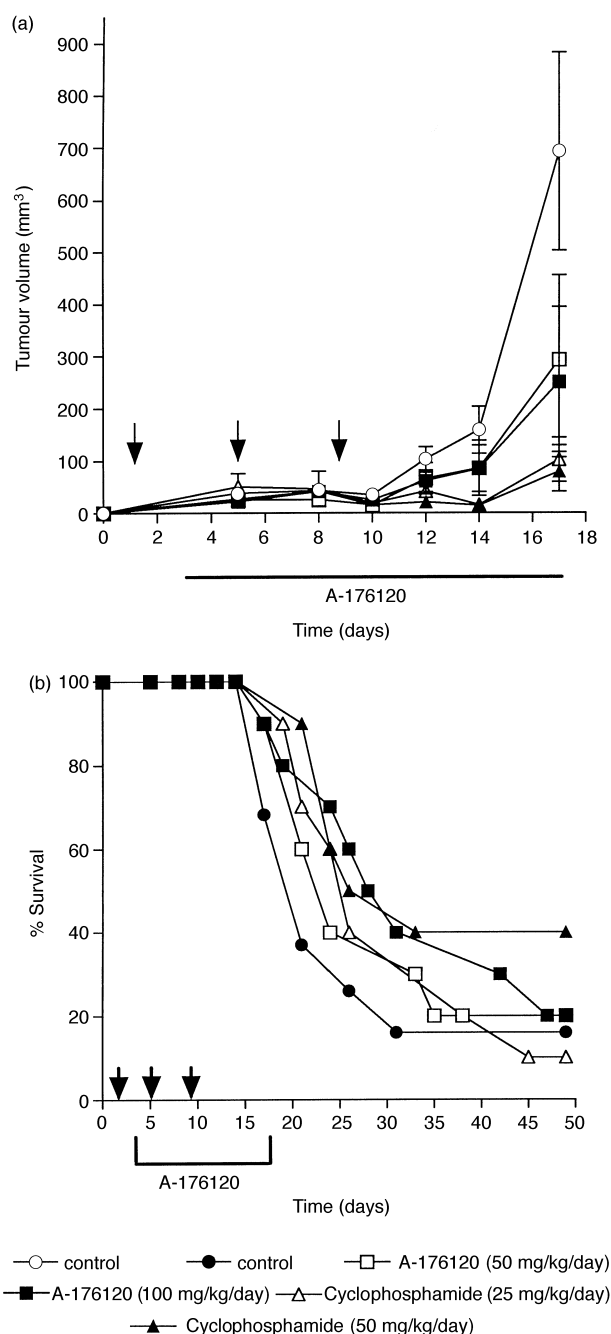


Fig. 7. A-176120 suppressed H-*ras*-transformed NIH3T3 tumour growth in nude mice. Mice were inoculated subcutaneously (s.c.) with tumour cells on day 0 and treated continuously with A-176120 intraperitoneally (i.p.) by minipump from day 3 to 17. Cyclophosphamide was administered by injection i.p. on days 1, 5 and 9. (a) Mean tumour volume±standard error. (b) Time for tumours to reach 1000 mm³ (~1 g). Tumour volumes were measured for up to 33 days following A-176120 treatment. Animals with tumours that reached or exceeded 1 g were euthanised. Statistical significance was determined using Student's *t*-test. Arrows, administration of cyclophosphamide on days 1, 5 and 9.

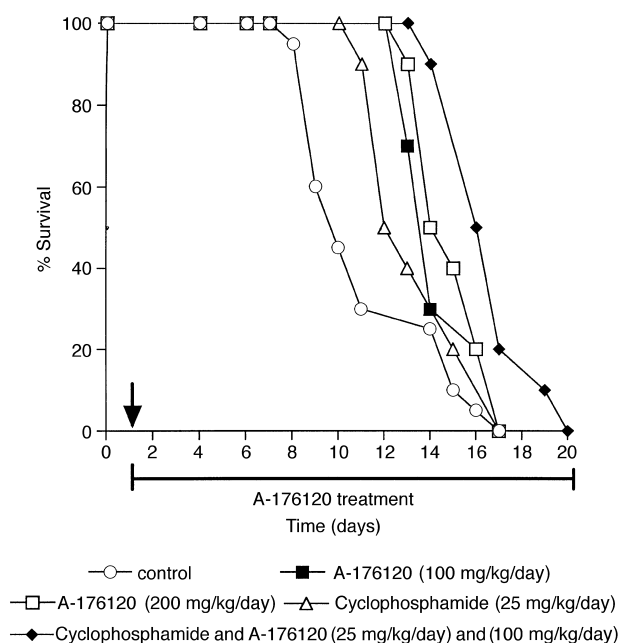


Fig. 8. A-176120 increased the lifespan of nude mice with *K-ras*-transformed NIH3T3 tumours. Mice were inoculated intraperitoneally (i.p.) with tumour cells on day 0 and treated continuously with A-176120 by minipump from day 1 to the end of the experiment. Cyclophosphamide was administered by injection i.p. on day 1. The mean survival time for each curve was used to determine the increase in lifespan. Statistical significance was determined using Student's *t*-test. Arrow, administration of 25 mg/kg cyclophosphamide on day 1.

potent in our series and the most potent FTI FPP mimetic reported to date. A-176120 inhibited FTase activity with IC_{50} values of 1.2 and 2 nM using K-Ras(B) decapeptide (KKSKTKCVIM) or H-Ras protein as substrates, respectively. The cellular ras processing IC_{50} values of A-176120 in H-*ras*-transformed NIH3T3 cells and K-*ras*-mutated HCT116 cells was 1.6 and 0.5 μ M, respectively. Moreover, the activity of A-176120 was 352- and 2500-fold more selective for FTase over the closely related enzymes GGTase I and GGTase II, respectively. One inherent disadvantage of using FPP mimetics is it serves as a substrate for FTase as well as other enzymes involved in the synthesis of squalene, dolichols, heme A and ubiquinones [20]. A potential side-effect to consider, therefore, was the non-selective inhibition of enzymes that use FPP as a substrate (i.e. SSase) in the biosynthesis of cholesterol. However, unlike some other FPP mimetics previously described [21] we demonstrated A-176120 did not inhibit SSase activity at concentrations in excess of 10 000 nM. In contrast to A-176120, α -hydroxyfarnesylphosphonic acid, another FPP mimetic, was reported previously to inhibit both FTase (IC_{50} value of 30 nM) and SSase activity (IC_{50} at 630 nM).

We demonstrated the *in vivo* efficacy of A-176120 against H- and K-*ras*-transformed cells and the additive effect of A-176120 in combination with cyclophos-

phamide. This is the first demonstration to our knowledge that a FPP mimetic FTI reduced the growth of K-*ras*-transformed tumours and had an additive effect with another anticancer therapeutic agent *in vivo*. Recently, Yonemoto and colleagues [22] demonstrated the *in vivo* efficacy of a FPP mimetic, J-104,871, which suppressed the growth of NIH3T3 H-*ras*-transformed tumours by 28 and 52% following 40 and 80 mg/kg/day treatment i.p. for 6 days. However, activity against the K-*ras*-transformed tumour or an additive effect with cytotoxic agents was not reported for J-104,871.

Since the potency of an FTI in cell culture and animal models does not always correlate with their *ras* mutational status (see review in Ref. [23]), the exact mechanism(s) of action of FTIs as antitumour agents remains open to debate. It is clear that FTI can inhibit farnesyltransferase activity, however, it is becoming less clear what contribution the effect of inhibiting Ras farnesylation contributes towards the antitumour efficacy of FTIs. Recent reports have suggested that the mechanism of action of FTIs may be multifactorial [17] involving other cellular targets such as Rho [23,24] or more than 50 other proteins that are now known to be farnesylated [25]. In addition, K-Ras can be geranylgeranylated in the presence of FTI, however, the biological significance of geranylgeranylated K-Ras is unclear [23,25]. Whether FTIs inhibit tumour growth through the inhibition of Ras function alone is not known. However, it has been shown repeatedly that FTIs can reduce tumour growth *in vivo* with little or no systemic toxicity [23] despite the fact that Ras plays an essential role for normal cell growth and differentiation [26,27].

With regard to the mechanism of action of A-176120, the reduction of tumour cell growth *in vivo* following treatment may be due to the direct suppression of tumour cell proliferation as was observed *in vitro*. However, others have previously shown that suppression of tumour cell proliferation alone may not adequately account for the fact that the effect of some FTIs *in vivo* is greater than that predicted *in vitro* [28]. One possibility is that A-176120 may induce cellular apoptosis. However, an induction of apoptosis *in vitro* was not observed following A-176120 treatment in anchorage-dependent cell growth conditions (data not shown). We tested the possibility that A-176120 may have anti-angiogenic properties since mutant *ras* has been shown to play a role in regulating the expression of VEGF in murine and human *ras*-mutated cell lines [19,29].

Our observation that A-176120 suppressed VEGF release by HCT116 cells, reduced HUVEC proliferation and ras processing and inhibited HUVEC tube formation *in vitro* suggested that A-176120 may exert its effect on tumour growth *in vivo*, at least in part, by suppressing tumour angiogenesis. We have previously shown that A-170634, a potent CAAX peptidomimetic FTI,

was able to affect angiogenesis *in vivo* [17] by reducing blood vessels in and around tumour xenografts and reducing blood vessel growth in a rat corneal angiogenesis model. A-176120 may act *in vivo* as an anti-angiogenic agent by directly interfering with the proliferation of endothelial cells during the process of angiogenesis through a Ras-mediated pathway. Alternatively, another direct mechanism may involve prenylated proteins such as RhoB that regulates the organisation of the cytoskeleton. The expression and organisation of the cytoskeleton plays an important role in endothelial cell migration and control of capillary growth during angiogenesis [30]. Previously, Prendergast and associates [31] have shown that FTI treatment could affect the actin cytoskeleton in normal and *ras*-transformed cells and suggested the effect could be mediated in part by affecting the function of farnesylated proteins, including RhoB. More recent studies support the hypothesis that RhoB plays an important role in FTI-mediated effects [24].

A-176120 may also act as an anti-angiogenic agent *in vivo*, indirectly, by modulating VEGF release from tumour cells. VEGF is important for stimulating endothelial cell growth, survival *in vivo* and cell migration [32,33]. Okada and colleagues [29] have shown that 3-fold suppression of VEGF expression in DLD-1 and HCT116 cells was sufficient to block tumour growth in nude mice. More recently it was shown that immature blood vessels in tumours may be sensitive to VEGF withdrawal. Benjamin and coworkers [34] demonstrated that loss of VEGF *in vivo* led to selective apoptosis of endothelial cells in immature vessels of glioma xenografts that had not yet recruited periendothelial cells.

Overall, our results have important implications since A-176120 may have pleiotropic inhibitory effects on tumour growth by inhibiting Ras post-translational processing in the tumour, as well as Ras-mediated VEGF angiogenesis. A-176120 may have utility as an effective therapeutic agent against tumours without *ras* mutations via its effect on angiogenesis which is presumably not dependent on the *ras* mutational status of the tumour. Prendergast and associates [35] have shown that tumour cells can develop resistance to FTIs *in vitro*. Presumably, such FTI-resistant cells *in vivo* should still be sensitive to FTIs acting through an anti-angiogenic mechanism. If A-176120 has a direct effect on genetically stable endothelial cells, then drug resistance should be less than if the effect was only on genetically unstable tumour cells [36].

In conclusion, the data presented here demonstrate the biological effects of A-176120 *in vitro* and *in vivo* and its potential as an anticancer therapeutic agent. A-176120 was a potent and selective FPP mimetic FTI *in vitro*. Of clinical significance we have shown A-176120 was effective against H- and K-*ras* tumours *in vivo* and that combination therapy of A-176120 with cyclophosphamide was additive.

References

- Hancock JF. Anti-Ras drugs come of age. *Current Biol* 1993, **3**, 770–772.
- Newman CMH, Magee AI. Posttranslational processing of the ras superfamily of small GTP-binding proteins. *Biochim Biophys Acta* 1993, **1155**, 79–96.
- Bollag G, McCormick F. Regulators and effectors of ras proteins. *Annu Rev Cell Biol* 1991, **7**, 601–632.
- Lowy DR, Willumsen BM. Function and regulation of ras. *Annu Rev Biochem* 1993, **62**, 851–891.
- Bos JL. ras Oncogenes in human cancer: a review. *Cancer Res* 1989, **49**, 4682–4689.
- Kiaris H, Spandidos D. Mutations of *ras* genes in human tumors. *Int J Oncol* 1995, **7**, 413–421.
- Boguski MS, McCormick F. Proteins regulating Ras and its relatives. *Nature* 1993, **366**, 643–654.
- Quilliam LA, Khosravi-Far R, Huff SY, Der CJ. Guanine nucleotide exchange factors: activators of the Ras superfamily of proteins. *BioEssays* 1995, **17**, 395–404.
- Barbacid M. Ras genes. *Annu Rev Biochem* 1987, **56**, 779–827.
- Hamilton AD, Sehti SM. Inhibitors of Ras farnesyltransferase as novel antitumor agents. *DN&P* 1995, **8**, 138–145.
- Gibbs JB, Oliff A, Kohl NE. Farnesyltransferase inhibitors: Ras research yields a potential cancer therapeutic. *Cell* 1994, **77**, 175–178.
- Qian Y, Sehti SM, Hamilton AD. Farnesyltransferase as a target for anticancer drug design. *Biopolymers* 1997, **43**, 25–41.
- Lerner EC, Hamilton AD, Sehti SM. Inhibition of Ras prenylation: a signaling target for novel anti-cancer drug design. *Anti-Cancer Drug Design* 1997, **12**, 229–238.
- Manne V, Ricca CS, Brown JG, et al. Ras farnesylation as a target for novel antitumor agents: potent and selective farnesyl diphosphate analog inhibitors of farnesyltransferase. *Drug Dev Res* 1995, **34**, 121–137.
- Harwood Jr HJ. Protein farnesyltransferase: measurement of enzymatic activity in 96-well format using TopCount microplate scintillation counting technology. *Analyt Biochem* 1995, **226**, 268–278.
- Agnew WS. Squalene synthetase. *Meth Enzymol* 1985, **110**, 359–373.
- Gu W, Tahir SK, Wang Y, et al. Effect of novel CAAX peptidomimetic farnesyltransferase inhibitor on angiogenesis *in vitro* and *in vivo*. *Eur J Cancer* 1999, **35**, 1394–1401.
- Plowman J, Dykes DJ, Hollingshead M, Simpson-Herren L, Alley MC. Human tumor xenograft models in NCI drug development. In Teicher B, ed. *Anticancer Drug Development Guide: Preclinical Screening, Clinical Trials, and Approval*. Totowa, Humana Press, 1997, 101–125.
- Rak J, Mitsuhashi Y, Bayko L, Filmus J, Sasazuki T, Kerbel RS. Mutant ras oncogenes upregulate VEGF/VPF expression: implications for induction and inhibition of tumor angiogenesis. *Cancer Res* 1995, **55**, 4575–4580.
- Goldstein JL, Brown MS. Regulation of the mevalonate pathway. *Nature (Lond)* 1990, **343**, 425–430.
- Gibbs JB, Pompliano DL, Mosser SD, et al. Selective inhibition of farnesyl-protein transferase blocks ras processing *in vivo*. *J Biol Chem* 1993, **268**, 7617–7620.
- Yonemoto M, Satoh T, Arakawa H, et al. J-104,871, a novel farnesyltransferase inhibitor, blocks Ras farnesylation *in vivo* in a farnesyl pyrophosphate-competitive manner. *Mol Pharm* 1998, **55**, 1–7.
- Lebowitz PF, Prendergast GC. Non-Ras targets of farnesyltransferase inhibitors: focus on *Rho*. *Oncogene* 1998, **17**, 1439–1445.
- Du W, Lebowitz PF, Prendergast GC. Cell growth inhibition by farnesyltransferase inhibitors is mediated by gain of geranylgeranylated RhoB. *Mol Cell Biol* 1999, **19**, 1831–1840.

25. Cox AD, Der CJ. Farnesyltransferase inhibitors and cancer treatment: targeting simply Ras? *Biochim Biophys Acta* 1997, **1333**, F51–71.
26. Johnson L, Greenbaum D, Cichowski K, et al. K-ras is an essential gene in the mouse with partial functional overlap with N-ras. *Genes Develop* 1997, **11**, 2468–2481.
27. Fox PL, Sa G, Dobrowolski SF. The regulation of endothelial cell motility by p21 ras. *Oncogene* 1994, **9**, 3519–3526.
28. Rak J, Filmus J, Finkenzeller G, Grugel S, Marme D, Kerbel RS. Oncogenes as inducers of tumor angiogenesis. *Cancer Metast Rev* 1995, **14**, 263–277.
29. Okada F, Rak JW, Croix BS, et al. Impact of oncogenes in tumor angiogenesis: mutant K-ras up-regulation of vascular endothelial growth factor/vascular permeability factor is necessary, but not sufficient for tumorigenicity of human colorectal carcinoma cells. *Proc Natl Acad Sci (Wash)* 1998, **95**, 3609–3614.
30. Ingber DE, Prusty D, Sun Z, Betensky H, Wang N. Cell shape, cytoskeletal mechanics, and cell cycle control in angiogenesis. *J Biomech* 1995, 1471–1484.
31. Prendergast GC, Davide JP, DeSolms SJ, et al. Farnesyltransferase inhibition causes morphological reversion of ras-transformed cells by a complex mechanism that involves regulation of the actin cytoskeleton. *Mol Cell Biol* 1994, **14**, 4193–4202.
32. Alon T, Hemo I, Itin A, Pe'er J, Stone J, Keshet E. Vascular endothelial growth factors act as a survival factor for newly formed retinal vessels and has implications for retinopathy of prematurity. *Nature Med* 1995, **1**, 1024–1028.
33. Criscuolo GR, Balledux JP. Clinical neurosciences in the decade of the brain: hypotheses in neuro-oncology. VEG/PF acts upon the actin cytoskeleton and is inhibited by dexamethasone: relevance to tumor angiogenesis and vasogenic edema. *Yale J Biol Med* 1996, **69**, 337–355.
34. Benjamin LE, Golijanin D, Itin A, Pode D, Keshet E. Selective ablation of immature blood vessels in established human tumors follows vascular endothelial growth factor withdrawal. *J Clin Invest* 1999, **103**, 159–165.
35. Prendergast GC, Davide JP, Lebowitz PF, Weshsler-Reya R, Kohl NE. Resistance of a variant ras-transformed cell line to phenotypic reversion by farnesyl transferase inhibitors. *Cancer Res* 1996, **56**, 2626–2632.
36. Kerbel RS. A cancer therapy resistant to resistance. *Nature* 1997, **390**, 335–336.